Near-surface imaging of the western part of the Kachchh Mainland Fault (KMF) using ground-penetrating radar (GPR), Kachchh Rift Basin, Western India

Mohamedharoon Shaikh[1], Soumyajit Mukherjee[1], D. M. Maurya[2], and L. S. Chamyal[2]*
[1]Department of Earth Sciences, Indian Institute of Technology Bombay, Powai, Mumbai-400076, Maharashtra, INDIA
[2]Department of Geology, The Maharaja Sayajirao University of Baroda, Vadodara-390002, Gujarat, INDIA

*E-mail: mhs_vad@yahoo.co.in

Keywords
Ground-penetrating radar; Kachchh Mainland Fault; Tectonics; Kachchh rift basin; Western India

Abstract
Ground-penetrating radar (GPR) investigations were conducted along the western part of the seismically active Kachchh Mainland Fault (KMF) of the Kachchh Rift Basin (KRB). The strike of the fault changes from NNW to W in the study area from Lakhpat in the west to Mundhan anticline in the east. The change in the strike is due to oblique-slip movement along various NNE-striking transverse faults cross-cutting the KMF. The GPR studies were conducted to precisely locate the surface position of the KMF and to understand its shallow subsurface geometry. The subsurface Interface Radar-20 (SIR-20) GPR system of GSSI Inc., USA along with 200 MHz frequency antenna were used. We infer the KMF to be a north-dipping normal to a near-vertical fault. The fault changes its attitude at places being affected by various transverse faults. The GPR data, along with the field evidence, such as fault zone deformational features– fault gouge, near-vertical dip of the competent lithology at the fault zone, shear, and baking effect of the lithology, have been found useful in locating the KMF and inferring its shallow subsurface geometry.

Introduction

The Kachchh Rift Basin (KRB), in Gujarat, on the western continental margin of India is undergoing active coseismic deformation (Maurya et al., 2017a; Shaikh et al., 2020, 2022). The KRB is controlled by W-striking intra-basinal faults- Kachchh Mainland Fault (KMF) (Shaikh et al., 2019, 2022; Maurya et al., 2022), Katrol Hill Fault (KHF) (Maurya et al., 2021; Tiwari et al., 2021), Island Belt Fault (IBF), South Wagad Fault (SWF) (Maurya et al., 2017b) and Gedi Fault (GF) (Fig. 1). The fault zones exhibit rugged hilly terrain with deformed Mesozoic rocks and lowlands filled with Neogene sediments and varying Quaternary sediment cover (Biwas, 1993). This study aims to precisely map the shallow subsurface trace of the western KMF, using ground-penetrating radar (GPR). The GPR has been proved as the most promising tool in imaging buried active faults and subsurface deformational structures in different geological settings (Carpentier et al., 2012; Ciniti et al., 2015).

Geological context

The KMF is the largest intra-basinal fault in the KRB, originating during the Mesozoic. It extends for over 150 km as a discontinuous north-facing scarp that defines the Northern Hill Range (NHR) in the upthrown block. The NHR is a fault-parallel flexure zone comprising asymmetric domes, anticlines, and drape folds (Shaikh et al., 2019). The downthrown block to the north comprises a Holocene sedimentary basin knows as the Banni-Great Rann (Biswas, 1993). The strike of the KMF changes from NNW to W due to lateral displacement caused by NNE-striking transverse faults, mostly located in the interdomal saddle zones. Several large magnitude earthquakes have occurred along the KMF, including the 1819 Allah bund earthquake (M_w 7.8), 1956 Anjar earthquake (M_w 6.1) and 2001 Bhuj earthquake (M_w 7.7) (Shaikh et al., 2022). The KMF acts as a lithotectonic contact between sub-vertical Mesozoic rocks, mostly sandstones, forming the northern limbs of the domes and steep Tertiary rocks (limestone, shale, clays, conglomerate) protruding from the Rann and alluvial sediments. The patchy fault exposures provide ground truth for interpreting the GPR data.

GPR survey methodology

GPR profiles from four sites (shown as 1–4 in Fig. 2) were analyzed to interpret the near-surface fault properties. The sites include southeast of the Karanpur dome (site 1), between Karanpur and Ghuneri dome (site 2), at Sahera and at the western flank of Mundhan anticline (sites 3 and 4). In most locations, the fault is buried under thin alluvial cover.

GPR investigations along the Kachchh Mainland Fault, Western India

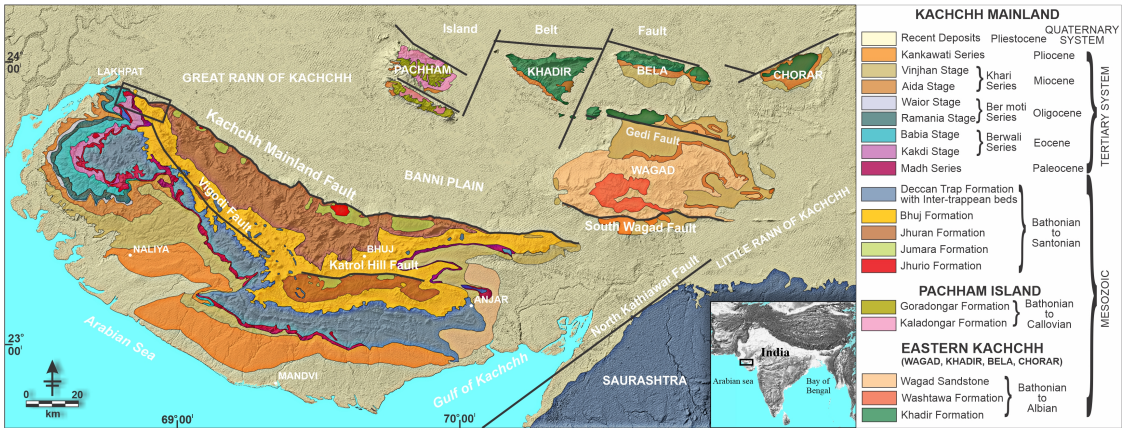

Figure 1: Geological map of the Kachchh Rift Basin (KRB) draped over shaded relief map derived from SRTM v.3 data. Geological and structural details are based on (Biswas, 1993). Inset- Shaded relief map of India showing location of the KRB marked by a solid rectangle. Box shows the area of present study.

Acquisition of geophysical data

Across-fault GPR surveys were conducted using shielded monostatic 200 MHz frequency antenna with a single-channel Subsurface Interface Radar-20 (SIR-20) system manufactured by GSSI Inc. USA. It provided satisfactory results in terms of penetration depth and resolution for studying the near-surface fault characteristics. The acquisition parameters are summarized in Table 1. Multiple profiles were collected along the same transect to determine the optimal header parameters. A manual marker was assigned to the profile at the inferred fault location to estimate its position. Changes in reflector patterns further confirmed the fault location. Common Mid-Point (CMP) gathers were acquired to estimate the electromagnetic wave propagation velocity.

Processing of GPR data

The raw GPR profiles were processed in RADAN (v.7) software by GSSI Inc. using standard processing steps to improve visualization and interpret geological features. Preprocessing is necessary due to noise, equipment instability, and vibrations during survey. The steps include- time-zero correction, topographic correction (except for one profile), horizontal scale normalization (stretching), background removal, band-pass filtering,

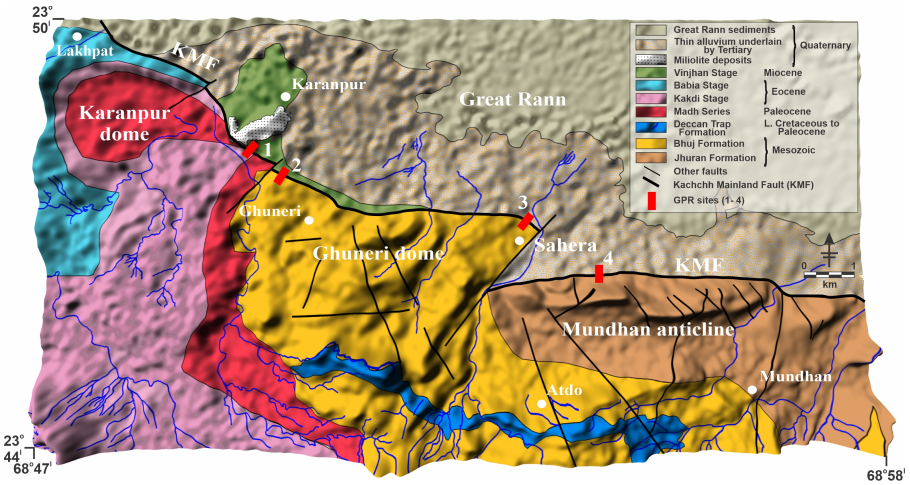

Figure 2: Structural map of the present study area with faults and rivers superimposed over shaded relief map derived from SRTM v.3 data. 1-4 are the ground-penetrating radar (GPR) survey sites.

GPR investigations along the Kachchh Mainland Fault, Western India

and gain restoration (Cassidy, 2009). Time-zero correction adjusted the vertical position, while a 2D background removal filter suppressed low-frequency noise. Vertical and horizontal band-pass filters were applied to eliminate unwanted noise, and gain restoration function normalized the gains. A horizontal low pass filter smoothed the profiles and removed vertical noise. Range gain function increased signal amplitudes and improved reflector visibility. CMP profiles were used for time-depth conversion and revealed a consistent subsurface velocity of 0.12 m/ns.

Survey parameters	Survey sites			
	Karanpur		Sahera	Mundhan
	Site 1	Site 2	Site 3	Site 4
Frequency (MHz)	200	200	200	200
Length (m)	21.5	50	35	37
Range (ns)	100	100	125	125
Attribute analysis	Trace envelope	Phase attribute + Trace envelope	Trace envelope	–

Table 1: Summarized data sheet of GPR survey acquisition and processing parameters for four sites.

GPR attribute analysis

Some profiles underwent additional processing using the Hilbert transform with Instantaneous Amplitude Envelope. This method calculates the absolute value of each wavelet, converting negative wavelets to positive mono-pulse wavelets (Dojack, 2012). It was used to detect energy loss in highly deformed fault zones based on signal strength and reflectivity. The results were more sensitive to detect the fault plane based on magnitude data rather than amplitude information. Superimposing trace envelope over wiggle trace and using phase attribute greatly improved the structural interpretation (Cinti et al., 2015). The instantaneous phase attribute highlights the discontinuity of reflectors in terms of faults, giving equal strength to weak and strong reflections.

GPR imaging interpretation

We analyze GPR profiles from four sites and discuss the results. The plot format varies, including wiggle trace overlapped by trace envelope, cosine phase attribute overlapped by trace envelope, and wiggle format alone, for more accurate depiction of data. In all cases, the fault zone is identified by the abrupt lateral change in amplitude, sudden truncation of reflectors, and areas of high energy loss (high signal

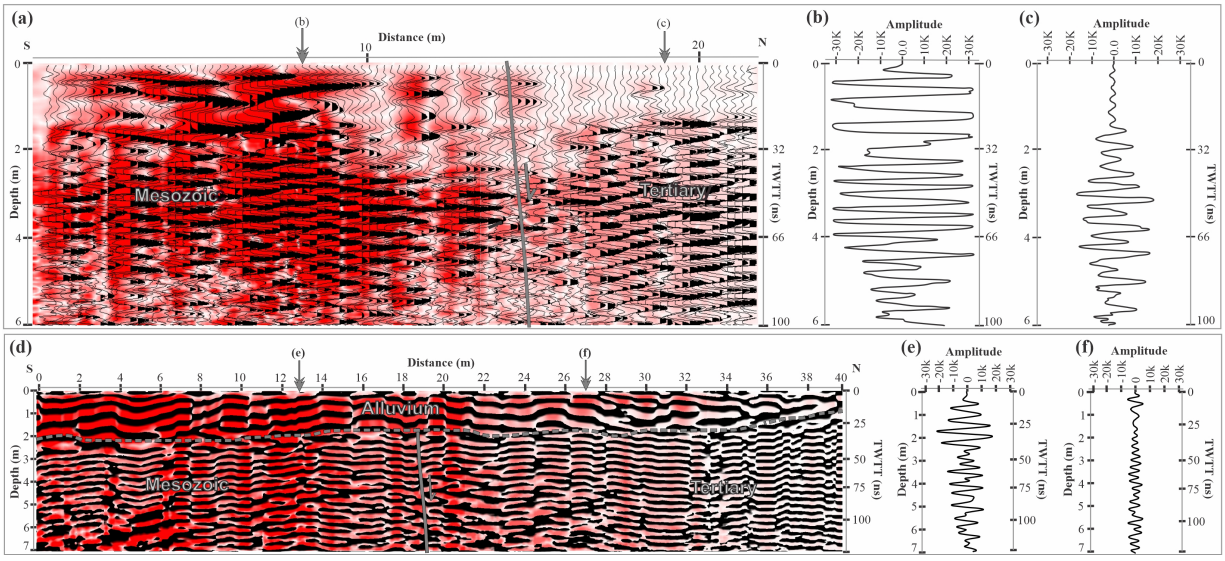

Figure 3: GPR profiles (a) trace envelope based on magnitude draped over wiggle traces recorded across the KMF, SE of Karanpur dome (site 1). Down arrows at the top of profile (marked as (b) and (c)) indicate the position of single scan in oscilloscope format. (b) and (c) show the individual waveform from Mesozoic rocks and Tertiary rocks, respectively. (d) trace envelope based on magnitude draped over trace envelope based on phase recorded across the KMF between Ghuneri dome and Karanpur dome (site 2). (e) and (f) show the respective single scans for Mesozoic and Tertiary rocks.

GPR investigations along the Kachchh Mainland Fault, Western India

attenuation) (Cinti et al., 2015).

Site 1

Site 1, located at SE of the Karanpur dome, exhibits N105º-striking sub-vertical nummulitic limestones of the Eocene and highly sheared Mesozoic sandstones (Fig. 2). The contact between the Mesozoic and Tertiary rocks marks the KMF. A 21.5 m long GPR transect was taken in N220º orientation, across the lithocontact (Fig. 3a). The interpreted profile depicts two distinct radar facies. The southern side shows high amplitude cycles with thick, horizontal reflections corresponding to compacted Mesozoic sandstones, while the northern side exhibits low, weak amplitude returns with successively increasing dip radar facies of Tertiary limestones (Figs. 3a–c). The Hilbert transform based on magnitude, overlapped on the wiggle trace, reveals ~5-7 m wide low-frequency anomaly indicating the presence of the fault zone (Fig. 3a). The fault zone exhibits poor reflection events, high signal attenuation, and a relatively "transparent" zone, likely due to intense lithological deformation causing significant energy loss. Both radar facies are truncated at the fault zone, indicating termination of strata. The KMF is marked by an abrupt amplitude decrease between the two sets of radar facies, at a distance of 14 m. It can be inferred that the KMF is a steep north-dipping normal fault at SE of Karanpur dome.

Site 2

Site 2, located NW of the Ghuneri dome, exposes N105º-striking sub-vertical nummulitic limestone of Eocene age (Fig. 2). Highly sheared, vertically dipping Mesozoic sandstones are also exposed. Both rock types are covered by patches of 1-2 m thick Quaternary alluvial deposits. The contact between the Mesozoic and Tertiary rocks is indicated by the fault gouge, cohesionless, unconsolidated, red powdery material that marks the KMF. The GPR profile shows the trace envelope using magnitude function overlapped with a trace envelope based on cosine phase (Fig. 3d). The southern side shows dense, strong amplitude reflections from the Mesozoic sandstones, while the northern side shows low, weak amplitude reflections from Tertiary limestones (Figs. 3d–f). The sudden truncation and dip change of continuous reflectors, and thinning-thickening of the reflections mark the KMF at ~20 m horizontal distance. The KMF is inferred to be a north-dipping normal fault NW of Ghuneri dome.

Site 3

At site 3, located near Sahera, the strike of the KMF changes to NNW due to strike-slip displacement along a NE-striking transverse fault (Fig. 2). The highly deformed, compact Mesozoic sandstones are exposed in patches at the southern side, while loose

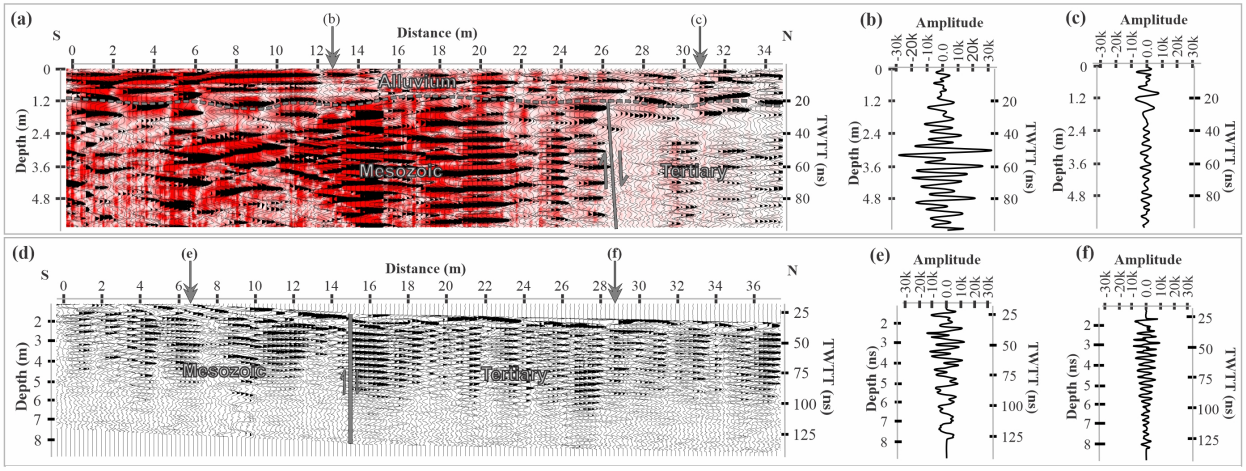

Figure 4: GPR profiles (a) trace envelope based on magnitude draped over wiggle traces recorded across the KMF, at Sahera (site 3). Down arrows at the top of profile (marked as (b) and (c)) indicate the position of single scan in oscilloscope format. (b) and (c) show the individual reflected waveform from Mesozoic rocks and Tertiary rocks respectively. (d) Wiggle traces recorded across the KMF at the western flank of the Mundhan anticline (site 4). (e) and (f) show the respective single scans for Mesozoic and Tertiary rocks.

GPR investigations along the Kachchh Mainland Fault, Western India

reddish clay representing Tertiary rocks is exposed to the north. ~35 m long GPR profile was collected from south to north (Fig. 4a). Strong, thick amplitude reflections can be identified, from ~2 m thick Quaternary sediment cover overlying the Mesozoic and Tertiary rocks. The compacted Mesozoic sandstone on the southern side exhibits northward dipping reflection patterns, while the Tertiary rocks show gently dipping to horizontal reflection patterns (Figs. 4a–c). The KMF is marked at ~26 m distance by observing the abrupt phase change in amplitude of the radar facies. This change is marked as the Mesozoic rocks show strong and wide amplitudes cycles whereas the Tertiary rocks show weak and small amplitude cycles (Figs. 4b, c). The reflections also die out at the fault plane.

Site 4

Site 4, located to the northern extremity of the Mundhan anticline, exposes near-vertical, W-striking, dark reddish, sheared, Mesozoic Jhuran sandstones, which approximate the position of the W-striking KMF (Fig. 2). To the south of the exposure, undeformed sandstone beds are exposed. To the east of this location, loose, partially compacted conglomerate of Paleocene age are exposed on the Rann surface. 37 m long GPR profile was acquired north of the scarp line, perpendicular to the fault strike. The raw GPR profile exhibited strong horizontal bands of ringing noise, which severely contaminated and masked the true reflections. To attenuate the reflections resulting from the ringing noise, the profile was processed according to the processing sequence proposed by Kim et al., 2007. Faulting was detected by observing the amplitude variations in the profile (Figs. 4d–f). The KMF is marked by an abrupt change in the amplitude at 15 m distance. The slip-sense of the fault is interpreted to be near-vertical based on the processed GPR profile.

Conclusions

High-resolution ground-penetrating radar (GPR) imaging along the western part of the Kachchh Mainland Fault (KMF) in the Kachchh Rift Basin (KRB) has provided critical data on the shallow subsurface fault geometry in the contemporary seismotectonic setting. Based on the GPR studies, we infer that the KMF is near-vertical at Mundhan anticline, which becomes a steep north-dipping normal fault near the Karanpur dome and Ghuneri dome. This tendency of the KMF to exhibit normal faulting is influenced by its proximity to the transverse faults in the study area.

Acknowledgements

MS acknowledges financial assistance from the Science and Engineering Research Board (SERB), Government of India, in the form of National Post-Doctoral Fellowship (NPDF) research project (No. PDF/2021/001644). Financial support from the Ministry of Earth Sciences (MoES), Government of India (project no. MoES/P.O.(Seismo)/1(170)/2013), to DMM and LSC is acknowledged.

References

Biswas, S., 1993, Geology of Kutch; K. D. Malaviya Institute of Petroleum Exploration, Dehradun, pp. 450.

Carpentier, S., Green, A., Doetsch, J., Dorn, C., Kaiser, A., Campbell, F., Horstmeyer, H., and Finnemore, M., 2012, Recent deformation of Quaternary sediments as inferred from GPR images and shallow P-wave velocity tomograms: Northwest Canterbury Plains, New Zealand, Journal of Applied Geophysics, 81, 2-15. https://doi.org/10.1016/j.jappgeo.2011.09.007

Cassidy, N., 2009, Ground penetrating radar data processing, modelling and analysis, In: H. Jol (Ed.), Ground Penetrating Radar Theory and Applications, Elsevier, New York; pp. 141-176. https://doi.org/10.1016/B978-0-444-53348-7.00005-3

Chowksey, V., Joshi, P., Maurya, D., and Chamyal, L., 2011, Ground penetrating radar characterization of fault-generated Quaternary colluvio-fluvial deposits along the seismically active Kachchh Mainland Fault, Western India; Current Science, 100, 915-921. https://www.jstor.org/stable/24076485

Cinti, F., Pauselli, C., Livio, F., Ercoli, M., Brunori, C., Ferrario, M., Volpe, R., Civico, R., Pantosti, D., Pinzi, S., Martini, P., Ventura, G., Alfonsi, L., Gambillara, R., and Michetti, A., 2015, Integrating multidisciplinary, multiscale geological and geophysical data to image the Castrovillari fault (Northern Calabria, Italy); Geophysical Journal International, 203, 1847-1863. https://doi.org/10.1093/gji/ggv404

Dojack, L., 2012, Ground Penetrating Radar Theory, Data Collection, Processing, and Interpretation: A

GPR investigations along the Kachchh Mainland Fault, Western India

Guide for Archaeologists, University of British Columbia Library, pp. 1-92. 10.14288/1.0086065

Kim, J., Cho, S., Yi, M., 2007, Removal of ringing noise in GPR data by signal processing, Geosciences Journal; 11, 75-81. https://doi.org/10.1007/BF02910382

Maurya, D., Chowksey, V., Patidar, A., and Chamyal, L., 2017a, A review and new data on neotectonic evolution of active faults in the Kachchh Basin, Western India: legacy of post-Deccan Trap tectonic inversion, In: S. Mukherjee, A. Misra, G. Calve's, M. Nemcok (eds.): Tectonics of Deccan large igneous province, 445th edn.; Geological Society of London Special Publication, London, 445, 237-268. https://doi.org/10.1144/SP445.7

Maurya, D., Chowksey, V., Shaikh, M., Patidar, A., Padmalal, A., Chamyal, L., 2022, Mapping the near-surface trace of the seismically active Kachchh Mainland Fault and its lateral extension in the blind zone, Western India. Near Surface Geophysics; 20, 544-566. https://doi.org/10.1002/nsg.12226

Maurya, D., Chowksey, V., Tiwari, P., and Chamyal, L., 2017b, Tectonic geomorphology and neotectonic setting of the seismically active South Wagad Fault (SWF), Western India, using field and GPR data, Acta Geophysica; 65, 1167-1184. https://doi.org/10.1007/s11600-017-0099-5

Maurya, D., Tiwari, P., Shaikh, M., Patidar, A., Vanik, N., Padmalal, A., Chamyal, L., 2021, Late Quaternary drainage reorganization assisted by surface faulting: The example of the Katrol Hill Fault zone, Kachchh, western India. Earth Surface Processes and Landforms; 46, 1268-1293. https://doi.org/10.1002/esp.5097

Shaikh, M., Maurya, D., Mukherjee, S., Vanik, N., Padmalal, A., Chamyal, L., 2020, Tectonic evolution of the intra-uplift Vigodi-Gugriana-Khirasra-Netra Fault System in the seismically active Kachchh rift basin, India: Implications for the western continental margin of the Indian plate. Journal of Structural Geology; 140, 104124. https://doi.org/10.1016/j.jsg.2020.104124

Shaikh, M., Maurya, D., Vanik, N., Padmalal, A., Chamyal, L., 2019, Uplift induced structurally controlled landscape development: example from fault bounded Jumara and Jara domes in Northern Hill Range, Kachchh, Western India. Geosciences Journal; 23, 575-593. https://doi.org/10.1007/s12303-018-0061-9

Shaikh, M., Patidar, A., Maurya, D., Vanik, N., Padmalal, A., Tiwari, P., Mukherjee, S., Chamyal, L., 2022, Building tectonic framework of a blind active fault zone using field and ground-penetrating radar data. Journal of Structural Geology; 155, 104526. https://doi.org/10.1016/j.jsg.2022.104526

Tiwari, P., Maurya, D., Shaikh, M., Patidar, A., Vanik, N., Padmalal, A., Vasaikar, S., Chamyal, L., 2021, Surface trace of the active Katrol Hill Fault and estimation of paleo-earthquake magnitude for seismic hazard, Western India. Engineering Geology; 295, 106416. https://doi.org/10.1016/j.enggeo.2021.106416